Cancer Research

The Transcriptional Regulatory Network of Proneural Glioma Determines the Genetic Alterations Selected During Tumor Progression

Adam M Sonabend, Mukesh Bansal, Paolo Guarnieri, et al.

Cancer Res Published OnlineFirst January 3, 2014.

The Transcriptional Regulatory Network of Proneural Glioma Determines the Genetic Alterations Selected During Tumor Progression

Running title: Phenotype-genotype interactions during proneural progression

Adam M Sonabend[1#], Mukesh Bansal[2,3#], Paolo Guarnieri[2,3], Liang Lei[4], Benjamin Amendolara[1], Craig Soderquist[4], Richard Leung[4], Jonathan Yun[1], Benjamin Kennedy[1], Julia Sisti[1], Samuel Bruce[1], Rachel Bruce[1], Reena Shakya[5], Thomas Ludwig[5], Steven Rosenfeld[6], Peter A Sims[2,7], Jeffrey N Bruce[1], Andrea Califano[2,3,7,8,9,10] and Peter Canoll[1,4*].

1) Gabriele Bartoli Brain Tumor Laboratory, Department of Neurosurgery, Irving Research Cancer Center, Columbia University Medical Center, New York, NY.
2) Department of Systems Biology, Columbia University, New York, NY
3) Center for Computational Biology and Bioinformatics, Columbia University, New York, NY
4) Department of Pathology and Cell Biology, Irving Research Cancer Center, Columbia University Medical Center, New York, NY.
5) Department of Molecular and Cellular Biochemistry, The Ohio State University Medical Center, Columbus, OH.
6) Brain Tumor and Neuro-Oncology Center, Cleveland Clinic, Cleveland, OH
7) Department of Biochemistry & Molecular Biophysics, Columbia University Medical Center, New York, NY.
8) Department of Biomedical Informatics, Columbia University, New York, NY.
9) Institute for Cancer Genetics, Columbia University, Columbia University, New York, NY.
10) Herbert Irving Comprehensive Cancer Center, Columbia University, New York, NY

Keywords: glioblastoma, transcription factor, proneural, deletion.

# These authors contributed equally
*Correspondent Author:

Peter Canoll, MD, PhD.
ICRC Room 1001
1130 St. Nicholas Ave
New York NY 10032
Phone: 212-851-4632
Fax: 212-305-4548
pc561@columbia.edu

The authors have no conflict of interest with the data presented on this manuscript.

Word count: 4999. Figures: 6. Supplementary Figures: 6. Supplementary Tables: 7. References: 44

ABSTRACT

Proneural Glioblastoma is defined by an expression pattern resembling that of oligodendrocyte progenitor cells, and carries a distinctive set of genetic alterations. Whether there is a functional relationship between the proneural phenotype and the associated genetic alterations is unknown. To evaluate this possible relationship, we performed a longitudinal molecular characterization of tumor progression in a mouse model of proneural glioma. In this setting, the tumors acquired remarkably consistent genetic deletions at late stages of progression, similar to those deleted in human proneural Glioblastoma. Further investigations revealed that p53 is a master regulator of the transcriptional network underlying the proneural phenotype. This p53-centric transcriptional network and its associated phenotype were observed at both the early and late stages of progression, and preceded the proneural-specific deletions. Remarkably, deletion of p53 at the time of tumor initiation obviated the acquisition of later deletions, establishing a link between the proneural transcriptional network and the subtype-specific deletions selected during glioma progression.

Abstract word count: 156

Precise: Perturbing a transcriptional network associated with glial progenitor transformation alters the course of glioma progression and prevents the selection of proneural-specific genetic alterations, demonstrating a functional interplay between tumor phenotype and genotype.

INTRODUCTION

Glioblastoma (GBM) is remarkably heterogeneous in genotype and phenotype, which constitutes a major challenge for targeted therapies (1-3). Whereas much of the diversity in GBM prognosis and clinical outcome has been attributed to its genetic heterogeneity, the determinants of such diversity remain obscure. Significant new evidence suggests that the acquisition of genetic alterations during tumor progression may be a deterministic rather than random process, influenced by multiple genetic and epigenetic factors (4-12). Thus, the phenotypic and genetic diversity of GBM might result from differences in the cell of origin (13, 14), age (11, 15), environment (5, 6) and/or pre-existent genetic background (4). Unfortunately, studying the factors that influence malignant progression is limited by poor reporting of relevant data in patient populations and by lack of data on cellular phenotype and genetic alterations in early stages of the disease.

Recent studies have revealed that GBM can be divided into distinct subtypes based on gene expression profiling, and that some subtypes are associated with a specific set of genetic alterations (14, 16), suggesting a functional relationship between phenotype and genotype. However, the mechanistic and temporal dependencies between tumor phenotype and its genotype remain elusive (3). The proneural subtype, in particular, is defined by a distinctive gene expression profile (GEP)(14), which resembles that of oligodendrocyte progenitor cells (OPCs), a presumed cell of origin for this group of gliomas (13). Proneural gliomas bear characteristic genetic alterations, such as TP53 and IDH1 mutations, as well as

PDGFRA amplification (14). The proneural phenotype is characteristic of the majority of low-grade gliomas, and secondary GBM (14). Thus, while proneural gliomas present with specific genetic alteration patterns, suggesting direct dependency between genotype and phenotype, the identification and characterization of causal events continues to elude us.

To address this question, we used a murine model of proneural glioma induced by overexpression of the PDGF oncogene, and inactivation of the Pten tumor suppressor (13). PDGF signals stimulate proliferation of oligodendrocyte progenitor cells (17, 18) and its overexpression has also been implicated as a driver of proneural gliomas (13, 14, 19, 20). In our model, tumor formation is induced by injecting PDGF-B-IRES-Cre (PIC) retrovirus into the subcortical white matter of adult *Pten*$^{lox/lox}$ transgenic mice (13). Thus, gliomagenesis starts as a small collection of retrovirus-infected glial progenitors and progresses to tumors that recapitulate the histological features of GBM with 100% penetrance. Cross-species comparison with human GBM from The Cancer Genome Atlas (TCGA) revealed that this model matches the proneural GEP signature (13).

In this study, we tracked the changes in gene expression, histological appearance, and gene copy number alterations that occur during initiation and progression of murine proneural gliomas. This allowed for phenotypic and genotypic characterization of tumor progression at different time points, with experimental control of variables such as age, cell of origin, environmental

exposures and genetic alterations. Our analysis showed remarkable consistency in the pattern of spontaneously occurring copy number alterations, including a subset of genes commonly deleted in both human and murine proneural tumors, thus establishing a temporal relationship between tumor phenotype and genotype. We also identified a proneural-specific transcriptional regulatory network in which p53 is a master regulator during both early and late stage glioma progression. Notably, upfront deletion of p53 facilitates glioma progression, without requiring accumulation of additional proneural specific deletions. These results provide experimental evidence for a functional link between the pre-existing cellular phenotype and the acquisition of specific genetic alterations.

METHODS

Tumor Models

The *PTEN$^{-/-}$, *PTEN$^{-/-}$p53$^{-/-}$ and *p53 tumors were generated by injecting PIC virus into the subcortical white matter of adult mice harboring floxed Pten or floxed p53, as previously described (13). For cell-transplantation experiments, 2X10^4 primary tumor cells were re-suspended in 2ul of Opti-MEM (Invitrogen) and injected into brain with flow rate at 0.2ul/min (n=20). Animals were followed, and upon signs of tumor-related morbidity were euthanized. Tumor DNA was collected at 21, 28 and 35 days post injection (dpi) for PDGF$^+$PTEN YFP$^+$ tumors, and upon death for PDGF$^+$PTEN$^{-/-\ luc+}$ and PDGF$^+$PTEN$^{-/-}$p53$^{-/-\ luc+}$ tumors (n=8 per group). RNA was isolated from 21 dpi PDGF$^+$PTEN$^{-/-}$ tumors, end-stage PDGF$^+$PTEN$^{-/-}$ and PDGF$^+$PTEN$^{-/-}$p53$^{-/-}$, as well as mouse frontal lobe specimens were also collected for

expression analysis (n=6 to 8 per group). All procedures were approved by the Institutional Animal Care and Use Committee of Columbia University.

Cell lines.

Ex-vivo gross resection of the tumor was performed and tumor cells were isolated using enzymatic digestion, (21, 22) and cultured overnight in media containing DMEM, N2, T3, 0.5% FBS, and penicillin/streptomycin/amphotericin,, PDGF-A (10 ng/ml) and FGFb (10 ng/ml) and B104 conditioned media (1:2) (23). Cell preparations were utilized for intracranial injection the following day. During these studies, we generated cell lines from *PTEN tumors and propagated them in culture as described (13, 24).

Comparative genomic hybridization.

Tumor and liver DNA was isolated (Qiagen DNA Mini Isolation Kit (51306) and Qiagen RNAse A (19101)) and paired for CGH analysis on the Agilent 244A Mouse Array CGH platform. Balanced dye swap was performed in 50% of the samples. Samples were corrected by subtracting the background; zeros and negative intensities were then set to half the minimum value of positive corrected intensities for the array. We performed a within array global median normalization and subsequent segmentation with smoothing using CBS [PMID:15475419]. Minimal common regions were called by means of Plink [PMID:17701901] using a 10 Kb windows size and 30% CNV overlap. We found that a gene that is deleted in (6/8) 75% of samples was significant for deletion ($p \leq 0.05$), compared to a random occurrence null hypothesis model. We compared *PTEN tumors against *PTEN/p53 with 50,000 sample permutations and an adjusted p-value $p \leq 0.05$ for significance.

Cre-mediated Pten deletion provides a validation of deletion differences between mouse tumor groups.

Given that comparisons made included tumors that were harvested through different techniques, and at different stages/sizes, we evaluated whether the relative tumor DNA content between these two cohorts was comparable. The log^2 ratio signal for tumor/non-tumor gene copy number for a probe that hybridizes the Cre/lox-mediated Pten deletion showed significantly lower Log^2 ratio for *PTEN 35 dpi tumors than either *PTEN or *PTEN/p53 end-stage tumors, suggesting a smaller fraction of tumor DNA on the former than the later groups, biasing against finding deletions in *PTEN 35 dpi tumors but not on *PTEN/p53 end-stage tumors (Supplementary Figure 1). Thus, it is unlikely that time alone can explain the difference in copy number alterations seen between these two models.

Cross-species Genomic Comparison.

For human gene copy number data acquisition, Affymetrix Genome-Wide Human SNP Array 6.0 data and Affymetrix U133A expression data for human GBM specimens (n=369) was querried available through the TCGA (http://cancergenome.nih.gov/). GBM subtypes were defined on the basis of expression profile using a classifier based on the subtypes previously described (14), and by a list kindly provided by Dr Verhaak (personal communication). Subgroup specific copy number gene alterations were defined by Chi square Test comparison between a subtype against the sum of all patients from the remaining three groups ($p<0.05$) with a false discovery rate <10%, and the presence of this deletion in at least 7% of that subgroup.

Trp53 DNA-based sequencing

Trp53 was sequenced following PCR amplification of exons 5-9 using genomic DNA as template. A second reverse sense confirmatory sequence for all positive samples was performed. Tp53 primers: Exon 5/6 FWD: 5'-CCGACCTCCGTTCTCTCTCC-3', REV: 5'-GTGAGGCAAACGGGTTGCTA-3', Exon 7 FWD: 5'-GGGAGCGACTTCACCTGGAT-3', REV: 5'-GGCAGAAGCTGGGGAAGAAA-3', and Exon 8/9 FWD: 5'-GATGGGGCCCAGCTTTCTTA-3', REV: 5'-TCTCTGGCATGCGACTCTCC-3'.

Cross-species comparisons of phenotype and transcriptional regulatory network analysis.

We prepared RNA-Seq libraries from each mouse normal brain (NB) or tumor sample and obtained 15-30 million single-end, 100-base reads on an Illumina HiSeq 2000 sequencer (JP Sulzberger Columbia Genome Center, NY). To assess the correlation with human GBM subtype designation (14), we calculated the Spearman's rank correlation coefficient using a previously described method for mouse RNA-Seq data (24). We use the median value of the correlation between an RNA-Seq data set and the TCGA microarray data for a given subtype as a similarity score for that subtype.

We applied ARACNe algorithm (25) to infer transcriptional regulatory network containing interactions between transcription factors and putative targets in human GBM using expression data for 319 samples obtained from TCGA (http://cancergenome.nih.gov). We interrogated the inferred network using the MARINa algorithm for master regulator analysis (25) to identify candidate master regulators (MR) that are likely to drive gene expression changes between proneural

GBM and human NB specimens. We identified MR using gene expression profiles from TCGA dataset and repeated the analysis on the Rembrandt glioma dataset (http://caintegrator-info.nci.nih.gov/rembrandt) to verify the consistency of identified MR. Molecular sub-class designation for human samples from TCGA and Rembrandt were obtained from prior publications (14, 16) and from personal communication from R.G. Verhaak. The same MARINa analysis was also performed on mouse transcriptional profiles, derived from RNA-Seq, by comparing NB GEP independently with profiles from *PTEN tumors at 21 dpi and end-stage. Statistically significant MARINa-inferred MRs ($p \leq 0.05$) were also analyzed based on the odd's ratio (OR) of their ARACNe-inferred genes, as previously defined (25). Transcriptional interactions in the regulatory network (Figure 4) were inferred by ARACNE. Raw data is available for download at http://www.ncbi.nlm.nih.gov/geo/.

RESULTS

Proneural Murine Gliomas Acquire Highly Consistent Gene Deletions During Tumor Progression.

To explore genetic and phenotypic changes related to glioma progression, cohorts of mice were sacrificed and analysed at different time points during glioma development. To evaluate small early stage lesions, *PTEN YFP^{+} tumors were used for fluorescence-guided micro-dissection. These tumors were generated by intracranial injection of PIC into Pten $^{lox/lox}YFP^{stop\text{-}flox}$ mice. At 21 dpi, *PTEN tumors had the histological appearance of low-grade gliomas. In contrast, end-stage *PTEN tumors had histological features of GBM, including glomeruloid vascular

proliferation, cellular atypia, and pseudopalisading necrosis. The later time point also showed a significantly higher Ki-67 labelling index ($p \leq 0.01$) (Figure 1A)(13).

We performed comparative genomic hybridization (CGH) of *PTEN tumors at dpi 21, 28, 35 and end-stage *PTEN (n=8 per time point). This analysis revealed a collection of copy number alterations, mostly deletions that increased in number over time, and were consistently seen at specific loci during later time points of *PTEN tumor progression (Figure 1B and C). *PTEN tumors acquired recurrent deletions with remarkable consistency, including 541 genes deleted in 75 to 100% of end-stage tumors (statistically significant by random permutation test, $p \leq 0.05$) (Supplementary Table 1). Copy number gains were also detected but were not as frequent as gene deletions (Figure 1C and Supplementary Table 2). At 21 and 28 dpi, *PTEN tumors acquired only a few copy number alterations, with overall frequency significantly lower than in end-stage *PTEN gliomas (Figure 1B and C). However, by 35 dpi, gene deletions were detected with similar frequency to end-stage *PTEN tumors (Figure 1C). Notably, CGH was able to detect the Cre-mediated deletion of Pten as early as 21 dpi (Supplementary Figure 1), arguing against the possibility that the differences in spontaneous deletions seen in early versus late stage tumors are merely due to changes in the fraction of retrovirus-infected tumor cells (harbouring Cre-mediated Pten deletion). Rather, these results support the conclusion that the spontaneous deletions are acquired in a subset of tumor cells and then selected for during tumor progression.

Cross-species Comparisons Identify Gene Deletions Common to Mouse and Human Proneural Gliomas.

To explore the similarities in the genetic alterations between mouse and human tumors, we compared the genes deleted in 75-100% of end-stage *PTEN tumors (n = 541) to gene deletions reported in the TCGA human GBM database (http://cancergenome.nih.gov). Furthermore, we assessed if there is a statistically significant bias in the distribution of the deletions across the 4 GBM subtypes (proneural, neural, mesenchymal and classical) (14). There were 108 genes that were deleted in 75-100% of end-stage *PTEN mouse tumors and deleted in greater than 10% of any human GBM subtype (Supplementary Table 3). Of these gene deletions, 75 were significantly and selectively enriched in the proneural subtype of human GBM ($p \leq 0.05$, FDR ≤ 0.1)(Figure 2A, Supplementary Table 4).

The 75 proneural-specific deleted genes clustered into 4 loci on human chromosomes 11p, 14q, 17p and 19q, all of which are within loci previously reported to be deleted in malignant gliomas (Figure 2B, Supplementary Figure 2, Supplementary Table 3)(26-28). When the threshold is relaxed to include genes deleted in more than 8% of any GBM subtype, an additional 17 genes are identified as being selectively deleted in proneural GBM, including 12 genes on chromosome 11q, 3 genes on chromosome 12q, and 2 genes on chromosome 19q (Figure 2B, and Supplementary Table 4). Using either of these thresholds, there were 3 genes on chromosome 10 that were significantly enriched in both the Classical and Neural subtypes and one gene on Chromosome 6 that was significantly deleted only in the

Classical subtype. Thus, in addition to the similarities seen at gene expression level (13), *PTEN tumors also most closely resemble the proneural subtype of human GBM in the pattern of genetic deletions that they acquire.

Interestingly the putative tumor suppressor gene CIC was deleted in 6/8 *PTEN 35 dpi and 5/8 *PTEN end-stage mouse tumors. Situated in the 19q locus in the human genome, CIC is often deleted or mutated in human oligodendrogliomas (29), as well as in 13.6% of proneural GBM from TCGA dataset.

Within the TCGA dataset, there were significant positive correlations among the proneural-specific deletions, including 17p with 11q ($p \leq 0.01$), and 17p with 14q deletion ($p \leq 0.05$) (Supplementary Table 5). We also compared the distribution of the proneural-specific deletions with other genetic alterations characteristic of proneural glioma, including PDGFRA amplification, TP53 mutations and IDH1 mutations, which coincide with a CpG island hypermethylation phenotype (14, 30). Deletion of 11q and 17p were overrepresented within proneural GBM patients bearing PDGFRA amplification ($p \leq 0.05$) and deletion of 11p and 19q were overrepresented within proneural GBM patients bearing IDH1 mutations ($p \leq 0.01$) (Supplementary Table 5), which in the case of 19q, resembles the scenario described in oligodendrogliomas (30, 31).

Proneural Phenotype Precedes the Accumulation of Genetic Deletions in Murine Gliomas.

*PTEN tumors show malignant progression including appearance of malignant histology and genetic alterations, but there is a clearly identifiable early stage in which these lesions are lacking such features. This allowed for direct investigation of the temporal relationship between genetic alterations and proneural phenotype during tumor progression. To evaluate whether the proneural phenotype precedes deletion of these genes, we performed RNA-Seq analysis of early and late stage tumors and used this data to classify tumor phenotype according to the Verhaak et al., gene set (14). We found that at 21 dpi, a time point that precedes the presence of highly recurrent gene deletions, murine gliomas already had higher resemblance to proneural glioma than to any other subgroup (Figure 3A). As shown previously (13), end-stage *PTEN tumors retained the proneural phenotype (Supplementary Table 6). Furthermore, differential gene expression analysis showed that OPC genes (32) that are part of the proneural gene set are significantly higher in both *PTEN 21 dpi and *PTEN end-stage in comparison to expression in NB specimens (Figure 3B). This is consistent with previous reports showing that early stage lesions in murine models of proneural glioma are composed of a massive expansion of OPC-like cells (13, 33). Thus, in this murine model, expression of a proneural signature precedes accumulation and selection of highly recurrent gene deletions, including those genes that are specifically deleted in human proneural GBM. This suggests that the proneural phenotype, which is characterized by the expression of OPC genes, provides the cellular context in which these specific genetic alterations are selected.

p53 is a Master Regulator of Proneural Transcriptional Network

To further characterize the proneural phenotype in which relevant deletions are selected, we used the MARINa algorithm (25). This analysis predicts transcription factors (TFs) that are master regulators (MRs) of the genes differentially expressed between two sample sets. Specifically, we used the algorithm to identify TFs whose ARACNe-inferred transcriptional targets are highly enriched in genes that are differentially expressed in 21 dpi, or end-stage *PTEN tumors compared to NB (Supplementary Table 7). Among these MRs, a few (*proneural MRs*) have ARACNe-inferred targets that are enriched in proneural signature genes compared to any other transcription factor in the genome ($p \leq 0.05$) (Figure 4A). Moreover, the proneural MRs form a densely connected transcriptional regulatory module among themselves and with other MRs identified by MARINa (Figure 4B). Notably, p53 was identified as a proneural MR of both early and late stage tumor progression. As such, it was found to interact with many other MRs in the transcriptional regulatory network (Figure 4).

To compare MRs of murine proneural progression with those driving human proneural GBM, we also used the MARINa algorithm to identify MRs whose targets are enriched in genes differentially expressed in human proneural GBM samples from TCGA versus NB (Supplementary Table 7). Findings from TCGA were highly consistent with those obtained by the MARINa analysis in an independent GBM dataset (Rembrandt, NCI) ($p \leq 1\text{x}10^{-35}$ by Fisher Exact Test). Cross-species comparison of murine and human MRs of proneural GBM showed a highly

statistically significant overlap ($p \leq 1x10^{-25}$, by Fisher Exact Test), as well a significant overlap between the ARACNe-inferred targets of the human and mouse MRs (Supplementary Figure 3, Supplementary Table 7). Notably, p53 is also identified as a MR of human proneural GBM. Thus, these analyses provide a putative regulatory context for the study of proneural gliomas, in which p53 and other TFs serve as MRs during different stages of tumor development.

An independent analysis was performed to identify potential upstream regulators of the genes differentially expressed between NB and end-stage *PTEN gliomas using the Ingenuity upstream regulator analysis (http://www.ingenuity.com/). This analysis also identified p53 as the most significant upstream transcriptional regulator ($p \leq 1x10^{-57}$). Thus, several independent analyses, across both murine and human gliomas, suggest that p53 plays an important role in the transcriptional regulation of the proneural subtype (Figure 4 and Supplementary Table 7).

Upfront Deletion of Trp53 Obviates Subsequent Proneural-specific Deletions During Glioma Progression

As discussed, regulatory analysis revealed p53 as a MR of the proneural transcriptional signature, at both early and late-stages of tumor progression, in *PTEN gliomas. Moreover, TP53 mutations are enriched within the proneural subtype of human GBM (14). Considering the well-established function of p53 as a tumor suppressor, these findings suggest p53 plays a central role in regulating the

growth of cells with a proneural phenotype. Furthermore, inactivation of p53, via direct mutations and deletions of the TP53 gene or via genetic alterations of other genes that are part of the p53 transcriptional network, will likely provide a powerful selective advantage to proneural glioma cells. If gene deletions in *PTEN end-stage tumors are functionally redundant to loss of p53, then upfront ablation of Trp53 should reduce the selective pressures to accumulate these deletions. To investigate this hypothesis, we analyzed the genome of a cohort of PDGF+PTEN$^{-/-}$p53$^{-/-}$ (*PTEN/p53) mouse tumors. These tumors have Trp53 loss as one of the initiating genetic alterations, since these are induced by intracranial injection of PIC into PTEN$^{lox/lox}$/p53$^{lox/lox}$ mice (13). The *PTEN/p53 tumors have a proneural expression pattern similar to that of *PTEN tumors, however the *PTEN/p53 tumors more rapidly progress to GBM (13). At 17 days post injection the *PTEN/p53 tumors were highly infiltrative and showed marked nuclear atypia and numerous mitotic figures (Supplementary Figure 4). By 21 days the tumors show the histological feature of GBM, including vascular proliferation and necrosis (Supplementary Figure 4).

Array CGH analysis across mouse tumor groups showed that end-stage *PTEN and *PTEN/p53 tumors had similar levels of Cre-mediated Pten exon 5 deletion, indicating that both tumor models were composed of a similar proportion of retrovirus infected cells (Supplementary Methods and Supplementary Figure 1). Gene copy number analysis revealed that *PTEN/p53 tumors accumulated gene deletions with a significantly lower frequency than *PTEN end-stage tumors (Figure

5) whereas gene amplifications occurred with a low frequency in both models (Figure 5 and Supplementary Table 2).

To rule out the possibility that differences in gene copy number alterations between end-stage *PTEN and *PTEN/p53 merely reflect the additional time for acquisition of these deletions, due to the difference in median survival between these two groups, CGH results were compared between end-stage *PTEN/p53 tumors and *PTEN tumors at 35 dpi, a time point that matched the end of the survival curve for mice bearing *PTEN/p53 tumors (n=8) (Figure 6A). Similar to the comparison with end-stage *PTEN, at 35 dpi *PTEN tumors had significantly higher frequency of gene deletions than *PTEN/p53 ($p \leq 0.05$) (Figure 5). Thus, time alone does not explain the difference in copy number alterations seen between these two models.

Murine Proneural Gliomas Acquire Alterations in p53 Pathway During Tumor Progression

*PTEN/p53 tumors had a significantly shorter survival than *PTEN lesions (13) (Log-rank $p \leq 0.01$) (Figure 6A). This difference in survival might reflect an inherently less aggressive phenotype for *PTEN tumors compared to *PTEN/p53. However, an alternative hypothesis is that the difference in survival may be due to the additional time required for *PTEN tumors to accumulate the additional genetic alteration needed for tumor progression, after which, *PTEN tumors grow as aggressively as *PTEN/p53 tumors. To directly compare the growth dynamics of

end-stage lesions of both tumor models, we transplanted $2X10^4$ cells from end-stage *PTEN or *PTEN/p53 into the brains of adult naïve mice, and in this case there was no significant difference in survival (Figure 6A). These findings, and the similar Ki-67 labelling (13), suggest that *PTEN tumor cells evolve over time into a more aggressive and proliferative phenotype, which, in the end-stage tumors, is comparable to that seen in *PTEN/p53 tumors.

Given the prominent transcriptional activity of p53 at different stages of *PTEN tumor development (Figure 4), we investigated the expression of transcriptional targets of p53 that are known to play a role in tumor suppression (34). Consistent with previous reports (13), a series of p53 targets had a significantly higher expression in *PTEN end-stage than on *PTEN/p53 tumors. Furthermore, our analysis of tumor progression in the *PTEN model shows that these transcriptional targets of p53 were highly up-regulated at early stages of tumor formation and then were significantly down regulated as the tumors progressed to end-stage (Figure 6B). This down-regulations coincided with the accumulation of deletions seen in *PTEN tumors, suggesting a possible functional relationship between the deleted genes and the expression of p53 and its targets. In support of this idea, Ingenuity-based analysis identified numerous previously described functional interactions between the gene deletions encountered in 75-100% of *PTEN tumors with p53 and/or its transcriptional targets that are established tumor suppressors (Figure 6C).

*PTEN tumors also acquired non-synonymous mutations in Trp53. Sanger sequencing analysis of Trp53 (exons 5 through 9) revealed that one third of the end-stage *PTEN tumors (n=5/15) had acquired missense mutations leading to a single amino acid substitutions within the DNA-binding domain of p53. Of note, all of these mutations were located in mutational "hotspots" in the p53 gene, which correspond to the most common mutations seen in human GBM (Figure 6D and Supplementary Figure 5) (35, 36). Previous studies have shown that these mutated alleles are expressed, but have abnormal transcriptional activity and loss of p53 tumor suppressor function (36). Examination of the RNA-Seq data of *PTEN end-stage tumors confirmed the transcription of the mutated allele in two cases that had paired RNA/DNA sequencing data. Sanger sequencing of 2 cell lines derived from *PTEN tumors also showed *Trp53* mutations, with the presence of a single peak, indicative of LOH with loss of the wild-type allele. Immunohistochemical analysis of one of these cells lines, which harbors a single mutant allele (R175H), showed nuclear staining for p53 (Supplementary Figure 5).

DISCUSSION

A key question within the field of cancer biology is the cause-effect and temporal relationship that exists between tumor phenotype and genotype, especially in cases in which a particular genetic alteration is associated with a specific phenotype. Here we showed that in a mouse model of proneural glioma, the proneural phenotype preceded the acquisition of highly specific gene deletions during tumor progression. Therefore, these genetic alterations occurred, and were

selected for, within the context of a pre-existing proneural phenotype. The fact that these genetic deletions were also commonly seen in human proneural GBM, suggests a functional link between genetic alterations and tumor phenotype that is conserved across species. Furthermore, we showed that in a highly controlled experimental setting, tumor evolution can be modelled with remarkable consistency, with spontaneous acquisition of some gene deletions in 75-100%. Our results also suggest that the selection of specific genetic alterations was influenced by initial conditions of gliomagenesis, which include the initiating genetic alteration and the cellular context in which these occur.

Deletion of Trp53 provided an experimental link between the proneural regulatory network and genetic alterations encountered in our model. Given that the proneural phenotype preceded the appearance of these gene deletions, the transcriptional regulatory network that drives this phenotype must be independent of these deletions. Nevertheless, this regulatory network had a strong influence on the selective pressure for these deletions during tumor progression. This point was illustrated by the fact that upfront deletion of Trp53, a highly interconnected MR transcription factor identified in the proneural regulatory network, accelerated tumor progression while obviating the selection of the highly recurrent deletions seen on the *PTEN tumor model. This finding suggests that there is a functional interplay between these genetic alterations and the intrinsic regulatory network.

p53 is highly active as a transcription factor at early and late stages of proneural glioma development, as evidenced by the elevated expression of p53 and its transcriptional targets in *PTEN 21 dpi, as well as in *PTEN end-stage lesions and human proneural GBM. These targets include the genes that constitute the proneural signature, as well as other proneural MR transcription factors (Figure 4). Notably, a subset of p53 targets that are implicated in tumor suppression are significantly down-regulated as the *PTEN tumors progress from 21 dpi to end-stage, and this is coincident with the accumulation of recurrent gene deletions observed during malignant progression. Moreover, these gene deletions did not occur when Trp53 was deleted as an initiating genetic lesion, suggesting functional redundancy.

Several previous studies have shown that deleting p53, in combination with other genetic alterations, will facilitate the formation of brain tumors (33, 37, 38). Similarly, we found that injecting PIC retrovirus into $p53^{lox/lox}$ mice induces tumors with the histological characteristics of GBM with 100% penetrance. The survival curve for the $PDGF^{+}/p53^{-/-}$ (*p53) model is significantly longer than that seen on *PTEN/p53 tumors, and significantly shorter than that seen on *PTEN tumors (Supplementary Figure 6). Similar to the *PTEN and *PTEN/p53 tumors (13), the *p53 tumors express high levels of glial progenitor markers and have a proneural phenotype (Supplementary Figure 6, Supplementary Table 6).

In addition to p53, several other MR identified in our analysis are known to play a role in glial progenitor biology and cancer. TCF3 inhibits the differentiation along the oligodendrocyte lineage, and regulates the cellular response to p53 in multiple cancers (39, 40). YY1, plays an essential role in oligodendrocyte progenitor differentiation, and has previously been identified as a regulator of the proneural-specific expression pattern in glioma (41, 42). E2F1 and E2F3, both identified as MR, promote cell cycle progression, and were previously found amplified in transgenic mouse models of glioma (38). MYC, a MR in both early and late stages of proneural glioma development, was previously implicated in self-renewal capacity and inhibition of differentiation in mouse glioma models, specifically in the context of loss of function of Pten and p53 (37).

In addition to this murine model, other groups have found that a variety models employing different genetic alterations can induce the formation of tumors that resemble proneural gliomas (13, 33, 38, 43). Chow et al., reported the genetic alterations in murine brain tumors, some of which had a proneural phenotype, induced by deleting various combinations of 3 tumor suppressors; Pten, Trp53 and Rb (38). CGH analysis showed that these tumors had accumulated frequent amplifications in Met, Pdgfra and Egfr, which are also commonly amplified in human GBM. In contrast, we did not observe amplifications of these growth factor receptors in our model (Supplementary Table 2). This difference might relate to the fact that in our model, glioma growth is driven by the retrovirus-induced PDGF-B expression, and this may obviate the need for amplification of oncogenes that provide additional

growth-promoting signals to the tumor cells. Interestingly, Chow et al. found large scale deletions of chromosomes 12 and 14 that overlapped with some of the deletions that were identified in our studies.

These studies demonstrate how cross-species comparison of cancer genomics provides a powerful approach to identify genes involved in tumorigenesis. This approach takes advantage of the phenotypic and genetic similarities between the mouse tumor models and human cancer, as well as the species-specific differences in genomic architecture and size of the copy number alterations. By doing this, we refined the list of thousands of genes deleted in human proneural GBM, to less than 100 genes that were specifically deleted in both mouse and human proneural tumors. Furthermore, some genes contained within a single deletion in human gliomas were distributed into multiple deletions on separate chromosomes in mouse gliomas, suggesting independent selection pressure for their loss (Supplementary Figure 2).

Our findings reveal non-random relationships between different genetic alterations in proneural GBM. These relationships included correlations of some of these deletions with established proneural-specific oncogenic genetic alterations (14), such as in the case of 11q and 17p with PDGFR amplification, or 11p and 19q with $IDH1^{R132}$ mutation, as well as correlations among the deletions that we encountered. These associations suggest a possible cooperation between tumor-promoting genetic alterations, with subsequent selection for their combination.

Understanding the forces and constraints that influence tumor evolution raises the possibility of new therapeutic interventions to manipulate this process towards a more indolent path. Such considerations are particularly relevant in setting of low grade gliomas, which have a strong tendency for malignant progression and which are mainly classified as proneural tumors (16, 30).

ACKNOWLEDGMENTS:

We acknowledge Rembrandt database from NCI and The Cancer Genome Atlas network researchers for providing the comprehensive human GBM database. We thank Dr. Roel Verhaak for the facilitation of proneural status for a list of TCGA patients. This work was funded by NIH/NINDS grant 1R01NS066955 (PC), Neurosurgery Research and Education Foundation (NREF) Award, AANS (AS), NIH/NIBIB grant 1K01EB016071 (PAS), and NIH R01 NS061776 (AC and MB).

REFERENCES

1. Network. CGAR. Comprehensive genomic characterization defines human glioblastoma genes and core pathways. Nature 2008;455:1061-8.
2. Parsons DW, Jones S, Zhang X, Lin JC, Leary RJ, Angenendt P, et al. An integrated genomic analysis of human glioblastoma multiforme. Science 2008;321:1807-12.
3. Zong H, Verhaak RG, Canoll P. The cellular origin for malignant glioma and prospects for clinical advancements. Expert review of molecular diagnostics 2012;12:383-94.
4. LaFramboise T, N. D, K. W, I. Pe, L. FM. Allelic selection of amplicons in glioblastoma revealed by combining somatic and germline analysis. PLoS Genet 2010;6.
5. Auger N, Thillet J, Wanherdrick K, Idbaih A, Legrier ME, Dutrillaux B, et al. Genetic alterations associated with acquired temozolomide resistance in SNB-19, a human glioma cell line. Mol Cancer Ther 2006;5:2182-92.
6. Dalton WS, Durie BG, Alberts DS, Gerlach JH, Cress AE. Characterization of a new drug-resistant human myeloma cell line that expresses P-glycoprotein. Cancer Res 1986;46:5125-30.
7. Dworkin AM, Ridd K, Bautista D, Allain DC, Iwenofu OH, Roy R, et al. Germline variation controls the architecture of somatic alterations in tumors. PLoS Genet 2010;6.

8. Gatenby RA, Brown J, Vincent T. Lessons from applied ecology: cancer control using an evolutionary double bind. Cancer Res 2009;69:7499-502.
9. Jonsson G, Naylor TL, Vallon-Christersson J, Staaf J, Huang J, Ward MR, et al. Distinct genomic profiles in hereditary breast tumors identified by array-based comparative genomic hybridization. Cancer Res 2005;65:7612-21.
10. Landi MT, Bauer J, Pfeiffer RM, Elder DE, Hulley B, Minghetti P, et al. MC1R germline variants confer risk for BRAF-mutant melanoma. Science 2006;313:521-2.
11. O'Regan EM, Toner ME, Smyth PC, Finn SP, Timon C, Cahill S, et al. Distinct array comparative genomic hybridization profiles in oral squamous cell carcinoma occurring in young patients. Head Neck 2006;28:330-8.
12. Stefansson OA, Jonasson JG, Johannsson OT, Olafsdottir K, Steinarsdottir M, Valgeirsdottir S, et al. Genomic profiling of breast tumours in relation to BRCA abnormalities and phenotypes. Breast Cancer Res 2009;11:R47.
13. Lei L, Sonabend AM, Guarnieri P, Soderquist C, Ludwig T, Rosenfeld S, et al. Glioblastoma models reveal the connection between adult glial progenitors and the proneural phenotype. PloS one 2011;6:e20041.
14. Verhaak RG, Hoadley KA, Purdom E, Wang V, Qi Y, Wilkerson MD, et al. Integrated genomic analysis identifies clinically relevant subtypes of glioblastoma characterized by abnormalities in PDGFRA, IDH1, EGFR, and NF1. Cancer Cell 2010;17:98-110.
15. Lee Y, Scheck AC, Cloughesy TF, Lai A, Dong J, Farooqi HK, et al. Gene expression analysis of glioblastomas identifies the major molecular basis for the prognostic benefit of younger age. BMC Med Genomics 2008;1:52.
16. Cooper LA, Gutman DA, Long Q, Johnson BA, Cholleti SR, Kurc T, et al. The proneural molecular signature is enriched in oligodendrogliomas and predicts improved survival among diffuse gliomas. PloS one 2010;5:e12548.
17. Besnard F, Perraud F, Sensenbrenner M, Labourdette G. Platelet-derived growth factor is a mitogen for glial but not for neuronal rat brain cells in vitro. Neurosci Lett 1987;73:287-92.
18. Westermark B, Wasteson A. A platelet factor stimulating human normal glial cells. Exp Cell Res 1976;98:170-4.
19. Huse JT, Holland E, DeAngelis LM. Glioblastoma: molecular analysis and clinical implications. Annu Rev Med 2013;64:59-70.
20. Brennan C, Momota H, Hambardzumyan D, Ozawa T, Tandon A, Pedraza A, et al. Glioblastoma subclasses can be defined by activity among signal transduction pathways and associated genomic alterations. PLoS One 2009;4:e7752.
21. Gensert JM, Goldman JE. Heterogeneity of cycling glial progenitors in the adult mammalian cortex and white matter. J Neurobiol 2001;48:75-86.
22. Mason JL, Goldman JE. A2B5+ and O4+ Cycling progenitors in the adult forebrain white matter respond differentially to PDGF-AA, FGF-2, and IGF-1. Mol Cell Neurosci 2002;20:30-42.
23. Canoll PD, Musacchio JM, Hardy R, Reynolds R, Marchionni MA, Salzer JL. GGF/neuregulin is a neuronal signal that promotes the proliferation and survival and inhibits the differentiation of oligodendrocyte progenitors. Neuron 1996;17:229-43.

24. Sonabend AM, Yun J, Lei L, Leung R, Soderquist C, Crisman C, et al. Murine cell line model of proneural glioma for evaluation of anti-tumor therapies. J Neurooncol 2013;112:375-82.
25. Lefebvre C, Rajbhandari P, Alvarez MJ, Bandaru P, Lim WK, Sato M, et al. A human B-cell interactome identifies MYB and FOXM1 as master regulators of proliferation in germinal centers. Molecular systems biology 2010;6:377.
26. Schiebe M, Ohneseit P, Hoffmann W, Meyermann R, Rodemann HP, Bamberg M. Loss of heterozygosity at 11p15 and p53 alterations in malignant gliomas. J Cancer Res Clin Oncol 2001;127:325-8.
27. Kitange G, Misra A, Law M, Passe S, Kollmeyer TM, Maurer M, et al. Chromosomal imbalances detected by array comparative genomic hybridization in human oligodendrogliomas and mixed oligoastrocytomas. Genes Chromosomes Cancer 2005;42:68-77.
28. Hu J, Pang JC, Tong CY, Lau B, Yin XL, Poon WS, et al. High-resolution genome-wide allelotype analysis identifies loss of chromosome 14q as a recurrent genetic alteration in astrocytic tumours. Br J Cancer 2002;87:218-24.
29. Bettegowda C, Agrawal N, Jiao Y, Sausen M, Wood LD, Hruban RH, et al. Mutations in CIC and FUBP1 contribute to human oligodendroglioma. Science 2011;333:1453-5.
30. Noushmehr H, Weisenberger DJ, Diefes K, Phillips HS, Pujara K, Berman BP, et al. Identification of a CpG island methylator phenotype that defines a distinct subgroup of glioma. Cancer Cell 2010;17:510-22.
31. Ducray F, Idbaih A, de Reynies A, Bieche I, Thillet J, Mokhtari K, et al. Anaplastic oligodendrogliomas with 1p19q codeletion have a proneural gene expression profile. Mol Cancer 2008;7:41.
32. Cahoy JD, Emery B, Kaushal A, Foo LC, Zamanian JL, Christopherson KS, et al. A transcriptome database for astrocytes, neurons, and oligodendrocytes: a new resource for understanding brain development and function. J Neurosci 2008;28:264-78.
33. Liu C, Sage JC, Miller MR, Verhaak RG, Hippenmeyer S, Vogel H, et al. Mosaic analysis with double markers reveals tumor cell of origin in glioma. Cell 2011;146:209-21.
34. Riley T, Sontag E, Chen P, Levine A. Transcriptional control of human p53-regulated genes. Nature reviews Molecular cell biology 2008;9:402-12.
35. Ohgaki H, Dessen P, Jourde B, Horstmann S, Nishikawa T, Di Patre PL, et al. Genetic pathways to glioblastoma: a population-based study. Cancer research 2004;64:6892-9.
36. Petitjean A, Mathe E, Kato S, Ishioka C, Tavtigian SV, Hainaut P, et al. Impact of mutant p53 functional properties on TP53 mutation patterns and tumor phenotype: lessons from recent developments in the IARC TP53 database. Human mutation 2007;28:622-9.
37. Zheng H, Ying H, Yan H, Kimmelman AC, Hiller DJ, Chen AJ, et al. p53 and Pten control neural and glioma stem/progenitor cell renewal and differentiation. Nature 2008;455:1129-33.

38. Chow LM, Endersby R, Zhu X, Rankin S, Qu C, Zhang J, et al. Cooperativity within and among Pten, p53, and Rb pathways induces high-grade astrocytoma in adult brain. Cancer Cell 2011;19:305-16.
39. Andrysik Z, Kim J, Tan AC, Espinosa JM. A genetic screen identifies TCF3/E2A and TRIAP1 as pathway-specific regulators of the cellular response to p53 activation. Cell reports 2013;3:1346-54.
40. Kim S, Chung AY, Kim D, Kim YS, Kim HS, Kwon HW, et al. Tcf3 function is required for the inhibition of oligodendroglial fate specification in the spinal cord of zebrafish embryos. Molecules and cells 2011;32:383-8.
41. He Y, Dupree J, Wang J, Sandoval J, Li J, Liu H, et al. The transcription factor Yin Yang 1 is essential for oligodendrocyte progenitor differentiation. Neuron 2007;55:217-30.
42. Setty M, Helmy K, Khan AA, Silber J, Arvey A, Neezen F, et al. Inferring transcriptional and microRNA-mediated regulatory programs in glioblastoma. Molecular systems biology 2012;8:605.
43. Pitter KL, Galban CJ, Galban S, Tehrani OS, Li F, Charles N, et al. Perifosine and CCI 779 co-operate to induce cell death and decrease proliferation in PTEN-intact and PTEN-deficient PDGF-driven murine glioblastoma. PLoS One 2011;6:e14545.
44. Kleihues P, Sobin LH. World Health Organization classification of tumors. Cancer 2000;88:2887.

Figure 1

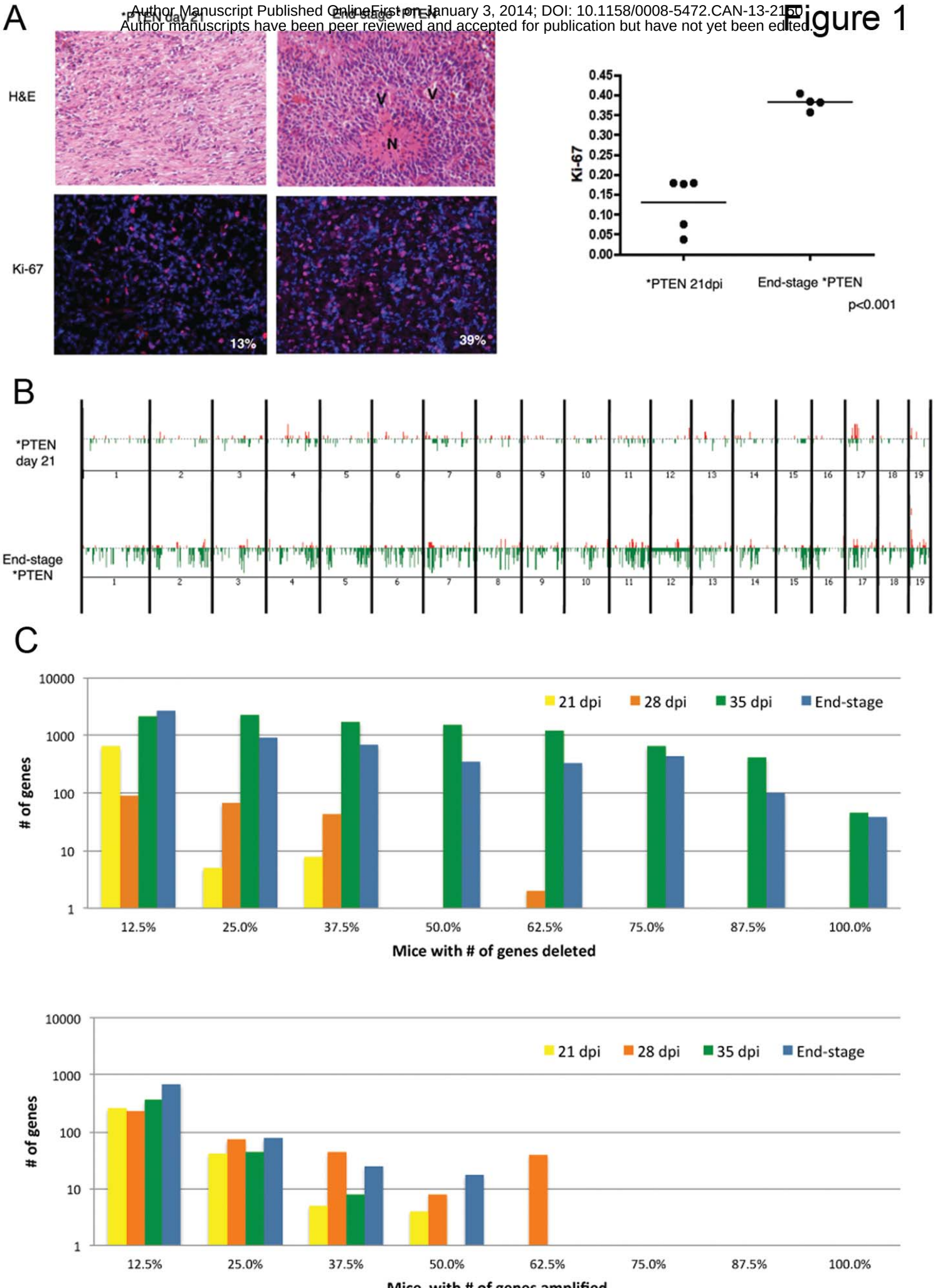

Author Manuscript Published OnlineFirst on January 3, 2014; DOI: 10.1158/0008-5472.CAN-13-2150
Author manuscripts have been peer reviewed and accepted for publication but have not yet been edited.

Figure 2

A

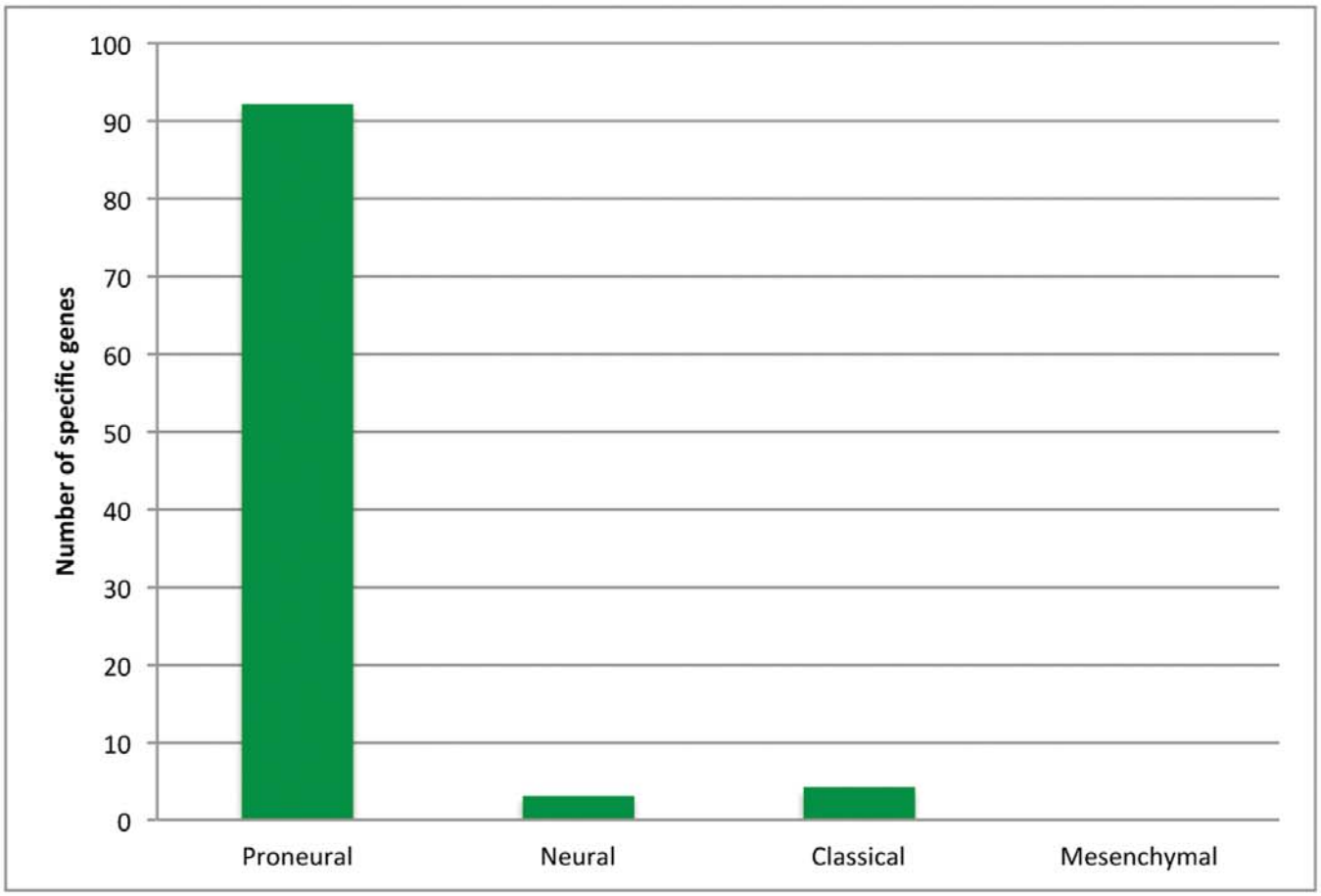

B

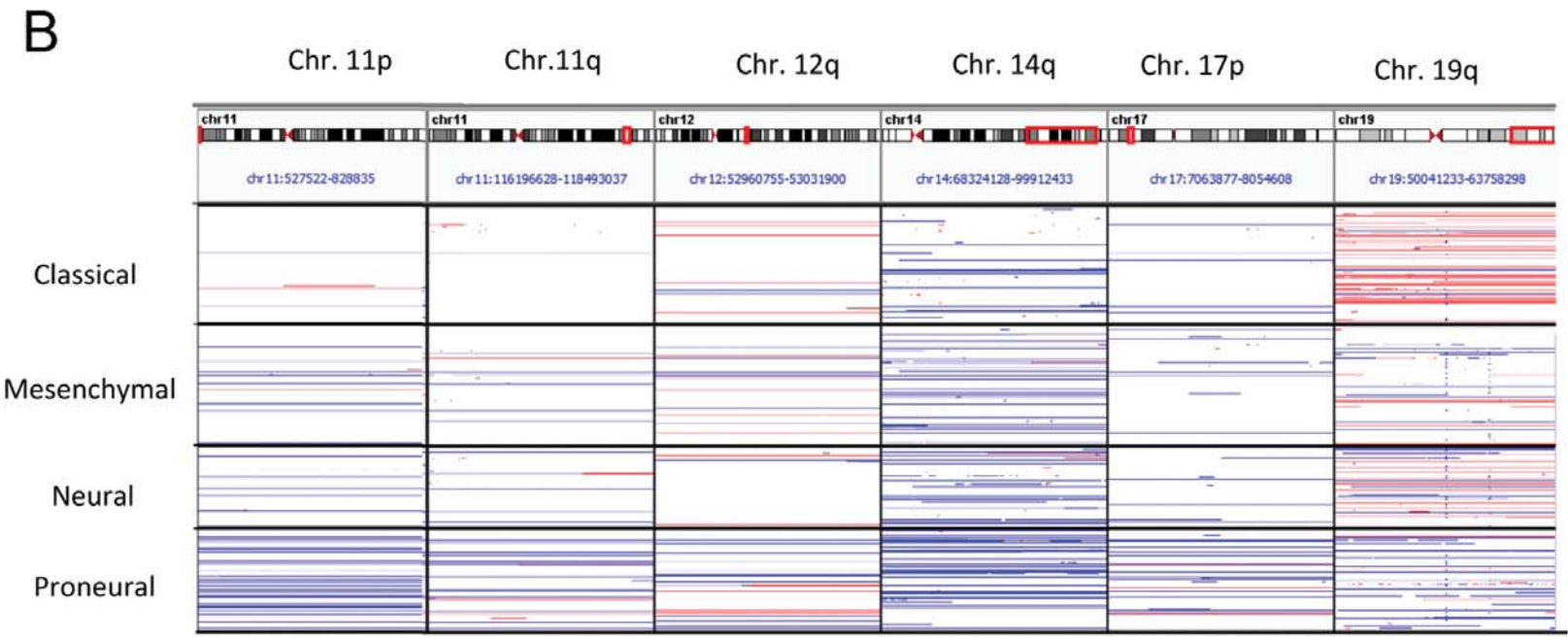

Figure 3

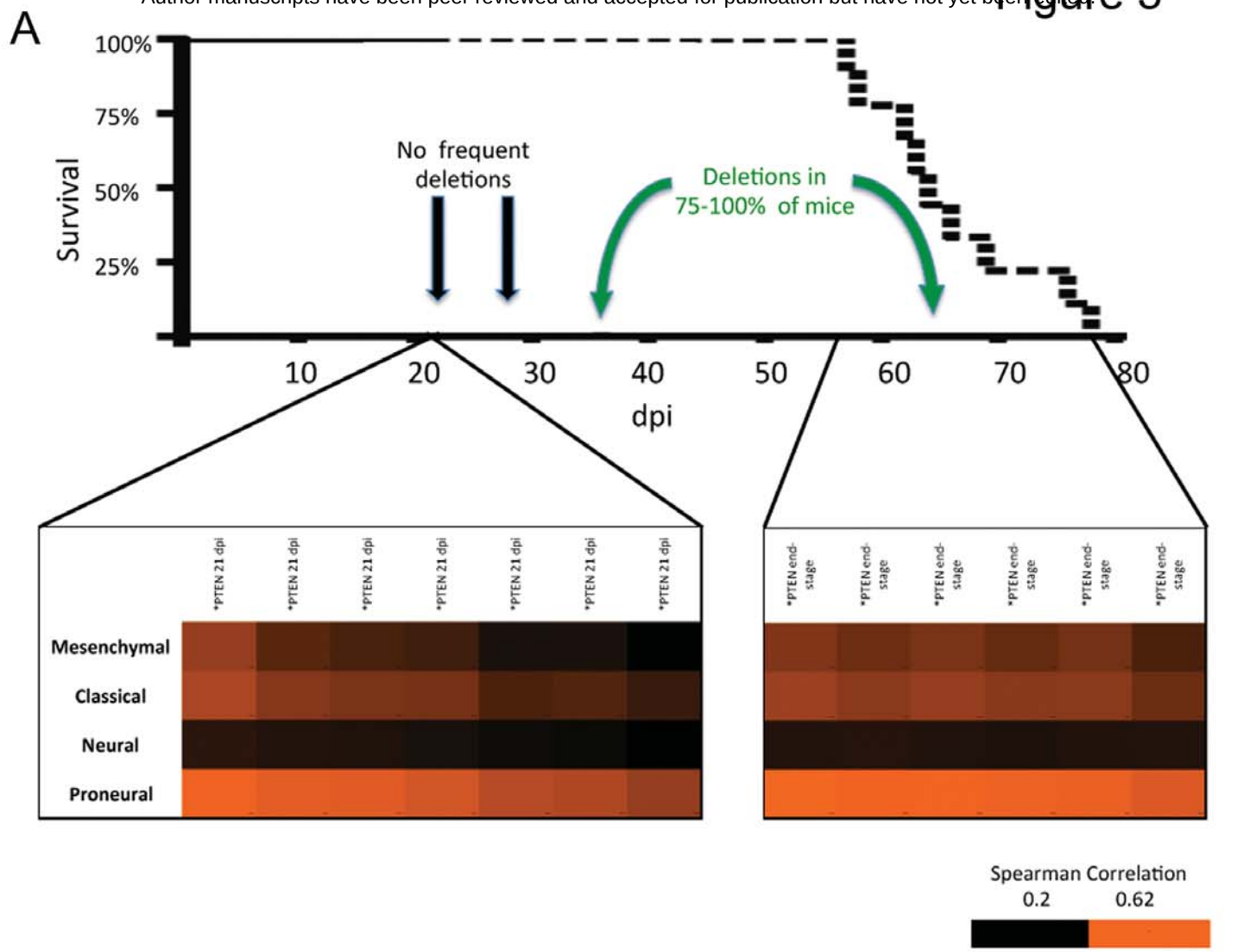

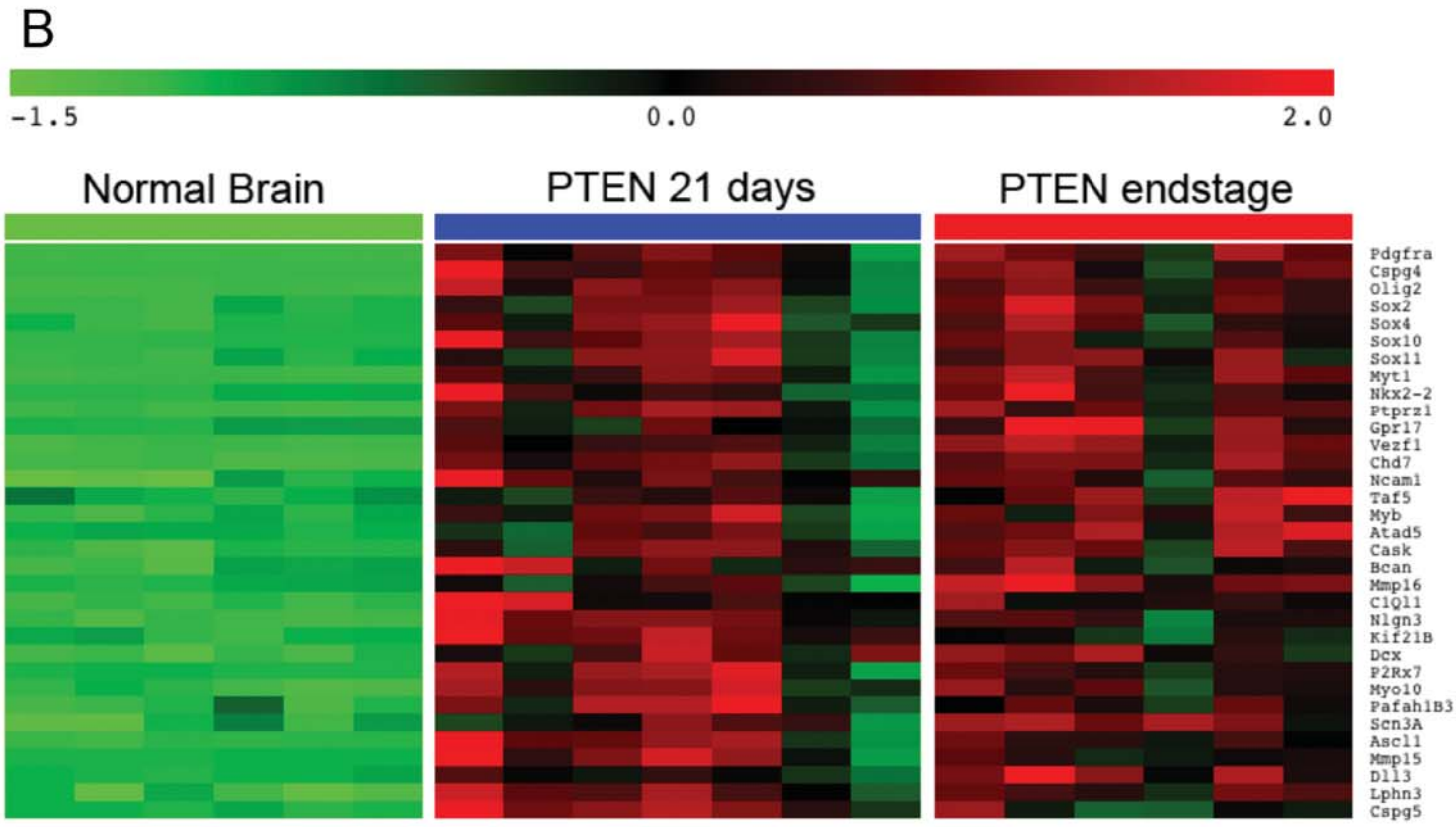

Figure 4

A

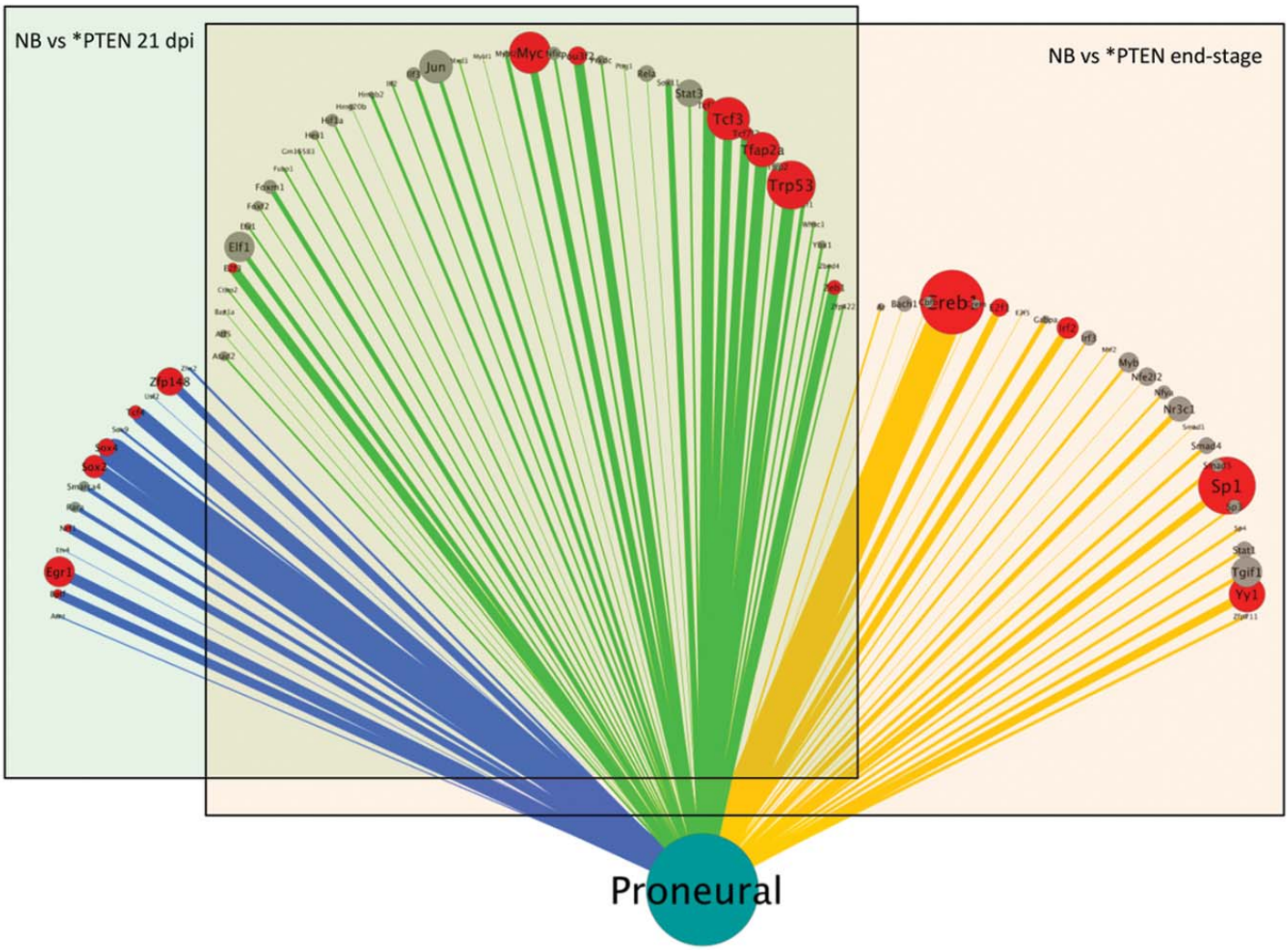

B

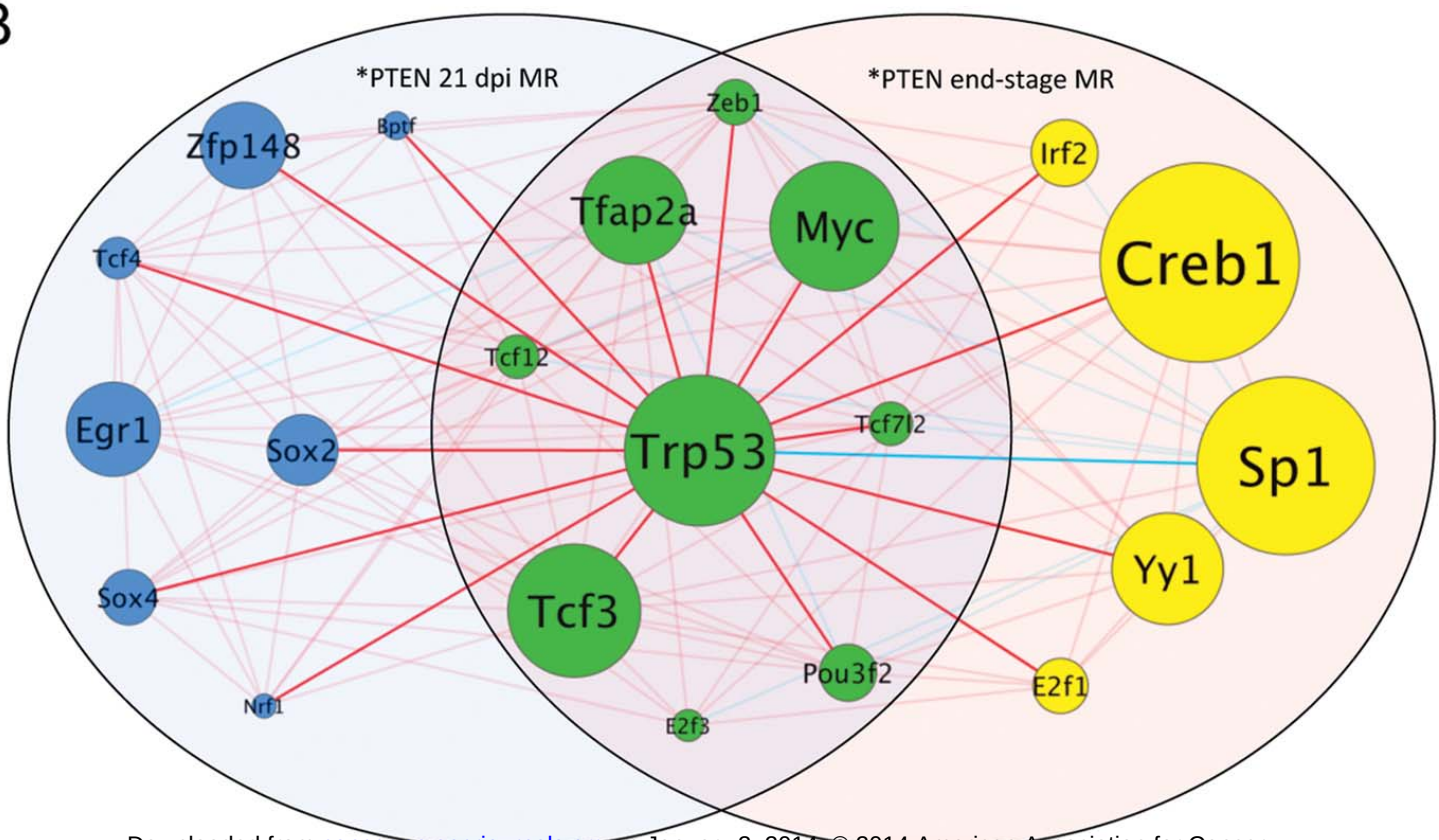

Figure 5

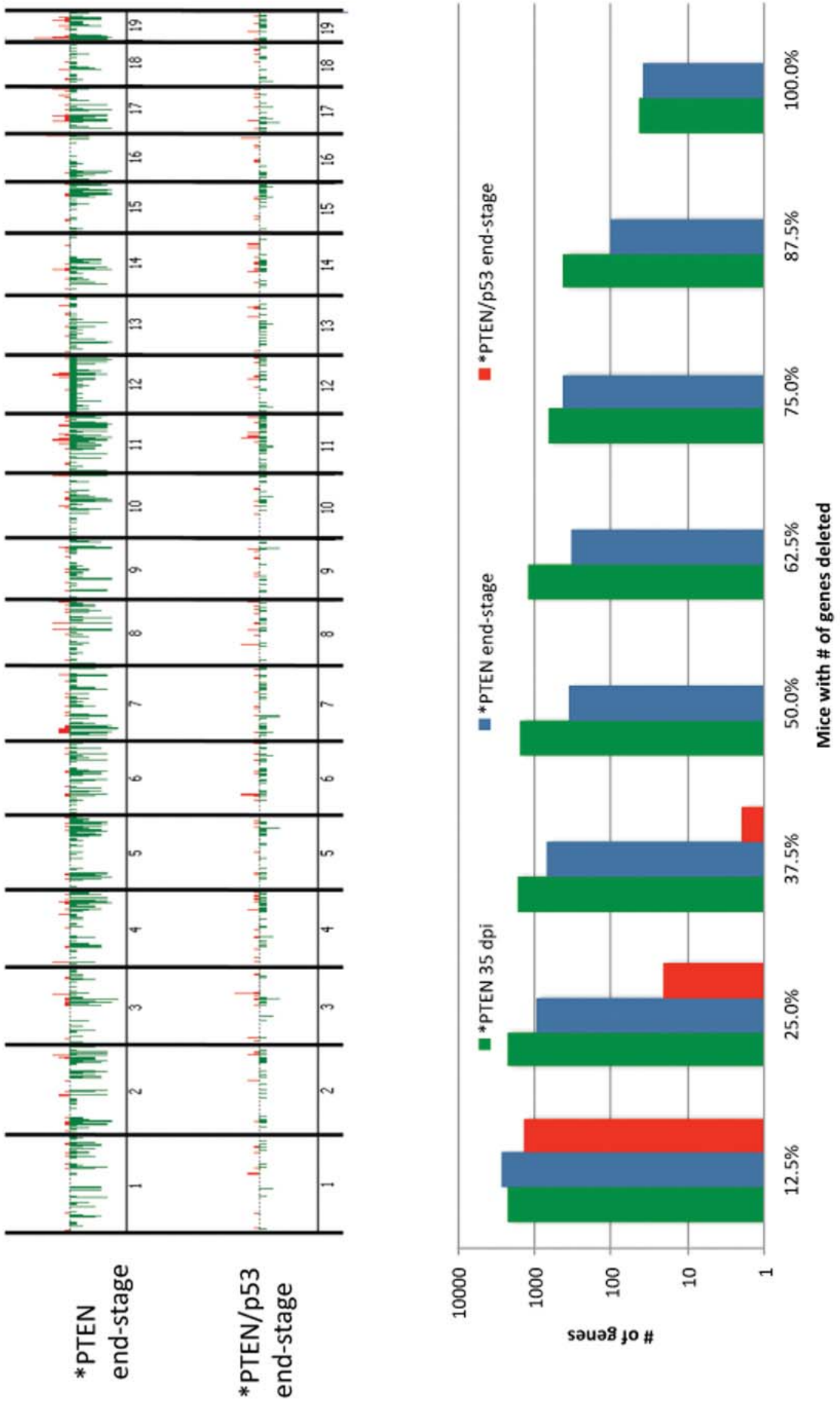

Author Manuscript Published OnlineFirst on January 3, 2014; DOI: 10.1158/0008-5472.CAN-13-2150
Author manuscripts have been peer reviewed and accepted for publication but have not yet been edited.

Figure 6